

This discussion paper is/has been under review for the journal Atmospheric Measurement Techniques (AMT). Please refer to the corresponding final paper in AMT if available.

Improving accuracy and precision of ice core $\delta D(\text{CH}_4)$ analyses using methane pre- and hydrogen post-pyrolysis trapping and subsequent chromatographic separation

M. Bock, J. Schmitt, J. Beck, R. Schneider, and H. Fischer

Climate and Environmental Physics, Physics Institute and Oeschger Centre for Climate Change Research, University of Bern, Sidlerstrasse 5, 3012 Bern, Switzerland

Received: 28 November 2013 – Accepted: 13 December 2013
– Published: 19 December 2013

Correspondence to: M. Bock (bock@climate.unibe.ch)

Published by Copernicus Publications on behalf of the European Geosciences Union.

Improving accuracy and precision of $\delta D(\text{CH}_4)$ analyses

M. Bock et al.

Title Page

Abstract

Introduction

Conclusions

References

Tables

Figures

⏪

⏩

◀

▶

Back

Close

Full Screen / Esc

Printer-friendly Version

Interactive Discussion



Abstract

Firn and polar ice cores offer the only direct paleoatmospheric archive. Analyses of past greenhouse gas concentrations and their isotopic compositions in air bubbles in the ice can help to constrain changes in global biogeochemical cycles in the past.

5 For the analysis of the hydrogen isotopic composition of methane ($\delta D(CH_4)$) 0.5 to 1.5 kg of ice was previously necessary to achieve the required precision. Here we present a method to improve precision and reduce the sample amount for $\delta D(CH_4)$ measurements on (ice core) air. Pre-concentrated methane is focused before a high temperature oven (pre pyrolysis trapping), and molecular hydrogen formed by pyrolysis is trapped afterwards (post pyrolysis trapping), both on a carbon-PLOT capillary at

10 $-196^\circ C$. A small amount of methane and krypton are trapped together with H_2 and must be separated using a short second chromatographic column to ensure accurate results. Pre and post pyrolysis trapping largely removes the isotopic fractionation induced during chromatographic separation and results in a narrow peak in the mass spectrometer. Air standards can be measured with a precision better than 1 ‰. For

15 polar ice samples from glacial periods we estimate a precision of 2.2 ‰ for 350 g of ice (or roughly 30 mL (at standard temperature and pressure (STP)) of air) with 350 ppb of methane. This corresponds to recent tropospheric air samples (about 1900 ppb CH_4) of about 6 mL (STP) or about 500 pmol of pure CH_4 .

20 1 Introduction

Methane (CH_4) is a potent greenhouse gas showing increased atmospheric concentrations since the industrial revolution (IPCC, 2007). A recent assessment of the present day methane budget is presented in Kirschke et al. (2013). However, the atmospheric load of CH_4 has varied on various time scales. A wealth of information has been

25 gained from concentration measurements regarding annual (Dlugokencky et al., 1995), decadal (Mitchell et al., 2011), millennial up to glacial/interglacial (Loulergue et al., 2008)

Improving accuracy and precision of $\delta D(CH_4)$ analyses

M. Bock et al.

Title Page

Abstract

Introduction

Conclusions

References

Tables

Figures



Back

Close

Full Screen / Esc

Printer-friendly Version

Interactive Discussion



**Improving accuracy
and precision of
 $\delta\text{D}(\text{CH}_4)$ analyses**

M. Bock et al.

Title Page

Abstract

Introduction

Conclusions

References

Tables

Figures

◀

▶

◀

▶

Back

Close

Full Screen / Esc

Printer-friendly Version

Interactive Discussion



CH₄ variability. Stable isotope data of methane on recent air samples (e.g. Quay et al., 1999) and on the past atmosphere using ice cores (e.g. Ferretti et al., 2005; Fischer et al., 2008; Sowers, 2010; Sapart et al., 2012; Möller et al., 2013) provide further insight into processes and sources controlling the global methane cycle. For instance, the temporal evolution of the hydrogen isotopic composition of methane ($\delta\text{D}(\text{CH}_4)$) over the termination of the last ice age (14 000–18 000 yr before present) (Sowers, 2006) as well as rapid warming events between 32 000–42 000 yr before present (Bock et al., 2010b) made it possible to reject the “clathrate gun hypothesis” proposed by Kennett et al. (2003) as the trigger for the steep atmospheric methane increases. Bock et al. (2010b) could also show that the precipitation signal ($\delta\text{D}(\text{H}_2\text{O})$), which changes from cold stadial to warm interstadial conditions, is traced into the paleo hydrogen isotopic signature of methane.

However, we are still far from a complete picture of the biogeochemistry of methane in the past. Ice core isotope studies on $\delta\text{D}(\text{CH}_4)$ have the potential to improve our understanding of the global CH₄ cycle but are still scarce due to analytical difficulties (e.g. Bock et al., 2010a; Sapart et al., 2011) and the large sample amount needed. To date the few published ice core $\delta\text{D}(\text{CH}_4)$ studies used 0.5 kg (Bock et al., 2010b) and more than 1 kg (Sowers, 2006, 2010; Mischler et al., 2009) of ice from multi parameter deep ice cores with a typical precision of around 3 to 4‰. This study presents new developments based on (Bock et al., 2010a) to improve precision and accuracy and reduce the sample size for (ice core) $\delta\text{D}(\text{CH}_4)$ measurements significantly.

2 Experimental

We present an improved continuous-flow gas chromatography (GC) pyrolysis (P) isotope ratio monitoring mass spectrometry (irmMS) system (GC/P/irmMS) designed to analyze $\delta\text{D}(\text{CH}_4)$ from (ice core) air samples (Fig. 1) with high precision. In the following we give a short summary of our previous instrumentation (Bock et al., 2010a) and new developments concerning the physical system and data processing.

**Improving accuracy
and precision of
 $\delta D(CH_4)$ analyses**

M. Bock et al.

Title Page

Abstract

Introduction

Conclusions

References

Tables

Figures

◀

▶

◀

▶

Back

Close

Full Screen / Esc

Printer-friendly Version

Interactive Discussion



The following steps are similar to Bock et al. (2010a): in a nutshell, a glass vessel containing an ice core sample is evacuated, and the enclosed air is released upon melting. In a high flow (He, 500 mL min⁻¹) water vapour is removed using a cooled Nafion membrane and a cold trap (T1) while the air sample is transferred to a trap filled with charcoal (T2) immersed in LN.

Contrary to Bock et al. (2010a), T1 is made up of an empty 1/8" tube of 3 coils that enter or leave a dewar maintained at -90 °C. Temperature controlled cooling of the dewar is achieved using LN droplets projected into the dewar (Schmitt, 2006; Bock et al., 2010a). T1 now removes only residual water vapour, while CO₂ is already adsorbed on an Ascarite trap, made of a 10 cm 1/4" stainless steel tube. In this new set-up N₂O is passed through the system to be measured in the mass spectrometer.

Air reference injections are realized by switching V1, either mimicking an ice sample by introducing the air into the glass extraction vessel or by bypassing the sample vessel, depending on the position of V2. Following a switch of V3, the air sample is transferred from the charcoal trap to a trap filled with Hayesep D (T3, at -100 °C), where methane is quantitatively trapped, while the bulk air (N₂, O₂, Ar) is vented. Residual air components and CH₄ are focussed on T4 (-196 °C) and injected onto a GC column. Valve V5 is switched to route the sample through a new cold trap (T5, -90 °C), replacing Nafion-2 of the old set-up, and towards the pyrolysis furnace only for the time window in which CH₄ is leaving the GC column.

In the following we describe the main new developments. Eluting CH₄ from the GC is focused on T6 for 18 s (pre pyrolysis trapping, prePT) before it is released by passive warming to room temperature. Subsequently, CH₄ is pyrolysed as described in Bock et al. (2010a), but the produced H₂ is not allowed to enter the mass spectrometer directly. Instead, H₂ is trapped on T7 for 40 s (post pyrolysis trapping, postPT). Both traps – T6 and T7 – are U-shaped, 20 cm long GC columns (GS-CarbonPLOT, ID 0.32 mm, film 1.5 μm, Agilent Technologies, part number 113-3112) retaining CH₄ and H₂ at LN temperature. After post pyrolysis trapping is complete, T7 is lifted out of LN and warmed to room temperature allowing H₂ to enter the mass spectrometer via an

Switzerland, DEGUSSIT[®] Al₂O₃, length = 420 mm, ID = 0.5 mm, OD = 1.5 mm) facilitates reproducible results for about four months. When a new reactor has to be installed, it is heated up using a ramp of 5 h and pre-conditioned over a day injecting 10 μ L loops every 3 min (without using any trap).

As a second major improvement to the system following a development by Schmitt et al. (2013b) we can now measure N₂O concentration, $\delta^{15}\text{N}$ and $\delta^{18}\text{O}$ of N₂O and xenon on the same sample. Therefore, after the H₂ acquisition for methane is completed, the pyrolysis reactor is bypassed using valve V6 and a peak jump is performed in order to tune the mass spectrometer to the N₂O configuration measuring m/z 44, 45, 46 using the triple collector. After a second peak jump we measure xenon (as ¹³²Xe²⁺ and ¹³⁶Xe²⁺) using beams m/z 66 and 68. Xenon is considered a proxy for total air content and is used to calculate CH₄ and N₂O concentrations. For detailed descriptions of N₂O and Xe analytic we refer the reader to a companion publication by Schmitt et al. (2013b) reporting on a new system to simultaneously measure $\delta^{13}\text{CH}_4$, isotopes of N₂O, Xe and other trace gas concentrations.

2.2 Data processing

We use custom made Python (<http://www.python.org/>) scripts to process the raw beam data, to organize peak data of reference, standards and samples in specific libraries and to perform the calibration to the international VSMOW (Vienna Standard Mean Ocean Water) scale. The peak integration method is similar to that described in Bock et al. (2010a). Integration limits are found based on the major beam time series and also applied to the minor beam. Instead of detecting the integration limits according to a slope threshold, we determine the peak maximum and set the peak start and end points to fixed numbers of data points before and after the peak maximum, i.e. we use a fixed peak width. In contrast to our previous procedure, pre&postPT removes the isotopic fractionation induced by the chromatographic separation resulting in nearly unfractionated H₂ peaks in the current set-up. Hence, we no longer perform a time

Improving accuracy and precision of $\delta\text{D}(\text{CH}_4)$ analyses

M. Bock et al.

Title Page

Abstract

Introduction

Conclusions

References

Tables

Figures

◀

▶

◀

▶

Back

Close

Full Screen / Esc

Printer-friendly Version

Interactive Discussion



shift correction of the m/z 3 beam, nor do we shift the left integration limit according to a peak size dependent value to correct for signal dependency as we did for our old system (Bock et al., 2010a). Generally, the background is determined as the median of the data points 6 s before the peak start (see Fig. 2).

In order to calibrate samples, it is essential to compare samples to standard measurements that are sufficiently stable over time and match the sample size. If this cannot be achieved, one has to correct for any drift and signal dependency (e.g. Schmitt et al., 2003; Potter and Siemann, 2004; Bock et al., 2010a; Brass and Röckmann, 2010). In our case this is essential, because we observe a clear signal dependency of the $\delta D(CH_4)$ values (Fig. 4). The signal dependency, however, is stable and reproducible over long time intervals and can therefore be precisely corrected for without compromising the overall precision of the measurement (see Sect. 3.2). When a new pyrolysis reactor is installed, the signal dependency changes, and a new interval of our data analysis has to be started to account for this change. We developed a new tool to correct for any system (time) drift and signal dependency at the same time, which is presented in detail in the appendix of this article. It takes standard measurements of known isotopic signature and iteratively fits parameters for (temporal) drift and signal dependency at the same time in order to minimize the standard deviation of $\delta D(CH_4)$ of our reference air. This assumes constant signal dependency within a certain time period (typically some weeks). The same assumption holds for laboratories determining signal dependency on a periodic schedule, but we see two advantages of our approach: (1) no extra day is needed to examine signal dependency and (2) if signal dependency changes slightly during the chosen time interval, this change is already accounted for by our standard measurements covering this interval. The fit parameters and daily mean values of our reference “Air Controlle” are used to calibrate the samples.

Improving accuracy and precision of $\delta D(CH_4)$ analyses

M. Bock et al.

Title Page

Abstract

Introduction

Conclusions

References

Tables

Figures



Back

Close

Full Screen / Esc

Printer-friendly Version

Interactive Discussion



3 System performance

3.1 Accuracy

Our reference used to calibrate all samples is “Air Controlé”, a recent clean air tank (CH_4 concentration = $[\text{CH}_4] = 1971 \pm 7$ ppb) for medical purposes (bottle 541659, filled February 2007 in Basel, Switzerland, Carbagas). “Air Controlé” was cross-referenced to -93.6 ± 2.2 ‰ with respect to Vienna Standard Mean Ocean Water (wrt VSMOW) using bottled air from Alert station “Alert 2002/11” (Bock et al., 2010a; Poss, 2003). According to thorough analyses performed at the University of Heidelberg, Germany, the Centre for Ice and Climate at the Niels Bohr Institute of the University of Copenhagen, Denmark and the Max Planck Institute in Jena, Germany, we are confident that our values exhibit a deviation from the VSMOW scale smaller than 3.5‰ (I. Levin, P. Sperlich, W. Brand, personal communication, 2013, and Sperlich et al., 2012).

We furthermore introduce a new standard gas here: “Saphir 4” (bottle 4405, Carbagas, artificial clean air mixture with 761 ppb CH_4 and no krypton) and ice core samples of a core dry drilled next to the EPICA (European Project for Ice Coring in Antarctica) drill site in Dronning Maud Land, Antarctica (EDML, $75^\circ 0.15' \text{S}$, $00^\circ 4.104' \text{E}$, 2892 m.a.s.l.), called “B34”. The air occluded in this ice has an approximate age of 1500 a BP.

Figure 6 shows $\delta\text{D}(\text{CH}_4)$ measured on B34 ice samples on a depth scale. The same data are also presented in Table 2, which additionally shows the measurement date and the weight of samples. Overall, we are confident that the described system was stable in terms of accuracy over the past few years. However, for polar ice samples (B34) it turns out that significant variations in $\delta\text{D}(\text{CH}_4)$ can occur within small depth ranges. Note for example the interval between 190 and 191 m where duplicates (samples from exactly the same depths) indicate good reproducibility, while going down core a depletion of several permil becomes obvious, which is significantly larger than the measurement error.

AMTD

6, 11279–11307, 2013

Improving accuracy and precision of $\delta\text{D}(\text{CH}_4)$ analyses

M. Bock et al.

Title Page

Abstract

Introduction

Conclusions

References

Tables

Figures

◀

▶

◀

▶

Back

Close

Full Screen / Esc

Printer-friendly Version

Interactive Discussion



**Improving accuracy
and precision of
 $\delta D(CH_4)$ analyses**

M. Bock et al.

Title Page

Abstract

Introduction

Conclusions

References

Tables

Figures

◀

▶

◀

▶

Back

Close

Full Screen / Esc

Printer-friendly Version

Interactive Discussion



Mean values for WAIS (Antarctica) and B30 (Greenland) from similar (pre industrial) time periods (around 410 and 670 a BP, respectively) are -73.0‰ and -91.5‰ ; hence, we estimate an inter polar difference of 18.5‰ with a combined error of 1.9‰ (the square root of the sum of the squared standard deviations of samples and reference measurements). This is a larger difference compared to the assessment by Sowers (2010), who reconstructed $12 \pm 6 \text{‰}$ for 550 to 960 a BP from the WAIS and GISP2 (Greenland Ice Sheet Project 2) ice cores, however still within the combined measurement uncertainties. Lower $\delta D(CH_4)$ values for the North are expected because high latitude methane emissions from boreal wetlands, thermokarst lakes and thawing permafrost are strongly depleted in deuterium and almost exclusively located in the Northern Hemisphere (Walter et al., 2008).

Saphir injections through the melt water of a previously extracted ice core sample are slightly depleted in deuterium (by 1.7‰) compared to Saphir injections bypassing the sample container, but the mean values are within the combined error. It is not clear whether this offset prevails for ice samples or if the effect only occurs after ice sample extractions. We therefore chose not to correct for this (potential) offset.

Note that our results for WAIS (West Antarctic Ice Sheet, core WDC05A, tube 184, depth range: 172.74–173.03 m, age approximately 410 a BP) are 15‰ more enriched in deuterium compared to data presented in Mischler et al. (2009). This offset is similar to the one observed for Boulder air (Bock et al., 2010a) compared to measurements performed at the Stable Isotope Lab of the Institute of Arctic and Alpine Research (INSTAAR, University of Colorado, Boulder, CO, USA) and shows that the laboratories in the US and Europe are tied to different primary standard air bottles. Note that no internationally accepted isotope reference material for CH_4 from air samples is yet available. At the time of writing, the mentioned lab offsets are being addressed in a round robin organized by T. Sowers and E. Brook using WAIS ice and bottled air samples with varying methane concentrations.

Post pyrolysis trapping and subsequent gas chromatographic separation enables the measurement of a pure H_2 peak in the mass spectrometer. Recently Schmitt et al.

(Table 1), which is now measured with a -5.8% offset and with a combined error of 3.5% (determined as above). Although this offset is still within 2σ of the error, we speculate that this is related to the Kr effect described above for measurements without post pyrolysis GC separation. The effect for Saphir is maximal as we standardize a non Kr and medium CH_4 containing sample (Saphir) with a standard containing recent Kr and CH_4 concentrations (“Air Controlé”) (see also Schmitt et al., 2013a). As our ice core samples also contain Kr, the effect is much smaller, as reflected in the very good correspondence of analyses with and without pre&post pyrolysis trapping and subsequent GC separation (Table 1).

3.2 Precision

In this section we describe the improvements concerning precision and sample size due to pre and post pyrolysis (pre&postPT) trapping of methane and hydrogen, respectively. In our old system (without pre&postPT) a typical sample (up to 500 g of polar ice with CH_4 concentrations between 350 and 700 ppb) showed peak heights of the major beam between 0.6 and 1.3 nA (for ice core samples presented in Bock et al., 2010b). While peak areas are still in the same range for identical amounts of CH_4 , major peak heights are increased roughly fourfold due to postPT. For B34 ice core samples between 200 and 450 g (with a CH_4 concentration of roughly 630 ppb), we now obtain peak heights between 1.5 and 4.3 nA. To mimic glacial low CH_4 content only 200–220 g samples of B34 ice (corresponding to 350–400 g with 350 ppb CH_4 as found for the last glacial maximum) were used and are listed in Table 2.

Table 1 summarizes our isotope results for air standards and ice samples. It is clear that precision of the new set-up is improved as indicated by smaller standard deviations of air standards (1.8% or better) and pooled standard deviations of ice core samples (2.3% or better), determined according to

Improving accuracy and precision of $\delta\text{D}(\text{CH}_4)$ analyses

M. Bock et al.

Title Page

Abstract

Introduction

Conclusions

References

Tables

Figures

◀

▶

◀

▶

Back

Close

Full Screen / Esc

Printer-friendly Version

Interactive Discussion



$$\sigma_p = \sqrt{\frac{\sum_{i=1}^k (n_i - 1)\sigma_i^2}{\sum_{i=1}^k (n_i - 1)}}$$

Note that the precision is comparable for small and large B34 samples (Table 2: e.g. samples < 220 g ice: $1\sigma = 2.1\%$). Based on the pooled standard deviation of B34 samples from the same depths, we estimate that our system's precision for ice samples is around 2.2%. Note that with this method $\delta D(\text{CH}_4)$ of present day tropospheric air can be measured with a precision better than 1% on 18–40 mL (STP) samples (Table 2).

We estimate that most of the gain in precision of the improved system is due to pre and postPT and only a small fraction can be attributed to our data processing routine. We assessed this by re-evaluating the standard measurements of our data set presented in Bock et al. (2010b) with the new python routine explained in the appendix. The standard deviation of all “Air Controlé” measurements using the new tool is 2.5% compared to 2.8% using the old procedure. Note, however, that even the smallest peaks of the old batch were larger by a factor of 1.6 compared to the tiny peaks that can now be measured with comparable precision using pre and post pyrolysis trapping. Furthermore, we acquired several runs of clean CH_4/He injections of varying methane amounts with and without pre&postPT as a second measure of the gain in precision. For the old system we obtained a standard deviation of 2.0% for peak areas between 1.8 and 13.3 nA. The smallest peaks between 1.8 and 3.0 nA could be measured with a precision of 2.6%. After introducing pre&postPT we are able to achieve a precision of 1.6% for even smaller peaks between 1.3 and 1.7 nAs. As seen for the re-evaluated “Air Controlé” measurements, for larger peaks the gain is smaller: indicated by a standard deviation of 1.4% for peak areas between 1.3 and 6.9 nAs. We conclude that the new data processing tool presented here represents an efficient and robust way to handle time drifts and signal dependency in one step but the main benefit considering precision is attributed to the implementation of pre and post pyrolysis trapping of methane and hydrogen, respectively.

Improving accuracy and precision of $\delta D(\text{CH}_4)$ analyses

M. Bock et al.

Title Page

Abstract

Introduction

Conclusions

References

Tables

Figures

◀

▶

◀

▶

Back

Close

Full Screen / Esc

Printer-friendly Version

Interactive Discussion



4 Conclusions

We presented pre and post pyrolysis trapping of methane and hydrogen, respectively, combined with post trapping GC separation on a PLOT column to improve accuracy and precision and reduce sample amount in $\delta D(CH_4)$ analysis of atmospheric and ice core samples. We showed that the precision for 350 g of ice (or roughly 30 mL of air) with 350 ppb of methane is approximately 2.2%. This corresponds to recent tropospheric air samples (roughly 1900 ppb CH_4) of about 6 mL (STP) or about 500 pmol of pure CH_4 . Vice versa 30 mL (STP) samples with recent tropospheric CH_4 concentration can be determined with a precision of better than 1%. Compared to our old set-up (Bock et al., 2010a) this translates into improvement factors for sample size (350 g)/(500 g) and precision (2.3 %)/(3.4 %) of 0.7.

We note, however, that the high standard in accuracy and precision for such small samples is achieved at the cost of measurement time; the new set-up allows the analysis of only one to two ice samples or four atmospheric samples a day.

We showed that potentially the accuracy of systems without pre&postPT and subsequent chromatographic separation can be biased depending on pyrolysis efficiency and varying methane/krypton ratios in samples and the reference. However, for atmospheric samples (preindustrial ice and air samples) the updated method did not measurably change in terms of $\delta D(CH_4)$ values compared to our initial set-up described in Bock et al. (2010a).

Appendix A

Correction for system drifts and signal dependency (linearity)

In order to calibrate samples measured on any isotope system, it is essential to compare samples to standard measurements that are sufficiently stable in time and match the sample size, or correct for any drift and signal dependency. As amount effects alter

AMTD

6, 11279–11307, 2013

Improving accuracy and precision of $\delta D(CH_4)$ analyses

M. Bock et al.

Title Page

Abstract

Introduction

Conclusions

References

Tables

Figures

◀

▶

◀

▶

Back

Close

Full Screen / Esc

Printer-friendly Version

Interactive Discussion



Improving accuracy and precision of $\delta D(\text{CH}_4)$ analyses

M. Bock et al.

Title Page

Abstract

Introduction

Conclusions

References

Tables

Figures

◀

▶

◀

▶

Back

Close

Full Screen / Esc

Printer-friendly Version

Interactive Discussion



isotopic results simultaneously with (time) drift effects, both errors should be corrected at the same time and not consecutively. A decoupling of the corrections is only possible when standards of constant peak size are measured to monitor the time trends only. Effects of signal dependency can be assessed by performing standard runs of different peak sizes, which is time consuming. Hence, we present an approach which allows simultaneous corrections of system drifts and signal dependency effects. For optimum conditions we choose size matching and bracketing standards for individual samples and pool standards measured over several days (assuming constant signal dependency over this time period) to cover the samples' size range. To correct for both signal dependency and drift effects, we use the following approach.

Any measured isotope value δX^{meas} is composed of the true value δX^{true} , any signal dependency, which is a function of peak area A , and a drift correction, which is a function of time t

$$\delta X^{\text{true}} = \delta X^{\text{meas}} - f^{\text{lin}}(A) - f^{\text{drift}}(t). \quad (\text{A1})$$

In the following, signal dependency is characterized by a polynomial of order N

$$f^{\text{lin}}(A) = \sum_{n=1}^N x_n A^n. \quad (\text{A2})$$

System drift is decomposed into two additive terms

$$f^{\text{drift}}(t) = f_1^{\text{drift}}(t) + f_2^{\text{drift}}(t). \quad (\text{A3})$$

The first term is a drift during a day, which is fitted to a polynomial of order M

$$f_1^{\text{drift}}(t) = \sum_{m=1}^M y_m t^m \Theta(t - [\bar{t}_i + \Delta t]) \Theta([\bar{t}_i - \Delta t] - t) \quad (\text{A4})$$

Improving accuracy and precision of $\delta\text{D}(\text{CH}_4)$ analyses

M. Bock et al.

Title Page

Abstract

Introduction

Conclusions

References

Tables

Figures

◀

▶

◀

▶

Back

Close

Full Screen / Esc

Printer-friendly Version

Interactive Discussion



dependent on time t . Therein t_i represents the time at day i the current sample was measured at. Thus, \bar{t}_i describes the mean measurement time of all samples measured during one day. Since temporal system drifts occur typically on time scales of weeks to months, the size of the drift within a day is usually small. Accordingly, our software allows for the calculation of $\delta\text{D}(\text{CH}_4)$ values with or without a diurnal drift correction (usually this is our preferred setting). The Theta-function Θ is zero, if its argument is < 0 and one if its argument is > 0 . This efficiently allows for the determination of the drift for each single measurement day in the program code. To discriminate between two adjacent laboratory days, Δt is defined as 0.4 days. The number of standard data points for each day should be larger but at least of the same size as M .

The second term represents the drift of the reference values between days. The mean isotopic reference signatures of all days are assumed to change in a stepwise linear fashion

$$f_2^{\text{drift}}(t) = \sum_{i=1}^L (m_i t + n_i) \Theta(\bar{t}_i - t) \Theta(t - \bar{t}_{i-1}), \quad (\text{A5})$$

where m_i quantifies the slope and n_i the intersection with the ordinate at a measuring day i , and L is the number of all measurement days.

Slope and intersection for each day i are calculated with respect to the previous day $i - 1$.

$$m_i = \frac{\bar{t}_i - \bar{t}_{i-1}}{\left[\delta X_i^{\text{meas}} - f^{\text{lin}}(A_i) \right] - \left[\delta X_{i-1}^{\text{meas}} - f^{\text{lin}}(A_{i-1}) \right]} \quad (\text{A6})$$

$$n_i = \left[\delta X_i^{\text{meas}} - f^{\text{lin}}(A_i) \right] - m_i \bar{t}_i. \quad (\text{A7})$$

Herein, influences of signal dependency have to be corrected for before calculating the mean standard isotopic signal of each day.

Improving accuracy and precision of $\delta D(CH_4)$ analyses

M. Bock et al.

Title Page

Abstract

Introduction

Conclusions

References

Tables

Figures

◀

▶

◀

▶

Back

Close

Full Screen / Esc

Printer-friendly Version

Interactive Discussion



We can express all quantities given in Eq. (A1) as functions of on peak area A and isotopic signature δX^{meas} at every measured point in time t . The true value of the standard δX^{true} is known. Thus, Eq. (A1) can be used to fit all measured data points. The fit parameters determine both the signal dependency and the drifts during and between the days by minimizing the standard deviation of all drift and signal dependency corrected standard values. The fitted parameters are then used to ultimately calibrate the samples by minimizing the standard deviation of all standard values.

Our routine is written in Python (www.python.org). The actual optimization uses the function `scipy.optimize.fmin()`. Figures 4 and 5 are produced by our routine and show uncalibrated and calibrated data, respectively. Each figure shows signal dependency in the left panel and time drift in the right panel.

Acknowledgements. Financial support for this study was provided in part by Schweizerischer Nationalfonds (SNF project primeMETHANE), and the European Research Council advanced grant MATRICs. We are grateful for B34 standard ice core samples provided by the Alfred Wegener Institute, Helmholtz Center for Polar and Marine Research. Many thanks to Willi Brand, Ingeborg Levin and Peter Sperlich for their help in evaluating lab offsets relative to the VSMOW scale.

References

- Bock, M., Schmitt, J., Behrens, M., Möller, L., Schneider, R., Sapart, C., and Fischer, H.: A gas chromatography/pyrolysis/isotope ratio mass spectrometry system for high-precision δD measurements of atmospheric methane extracted from ice cores, *Rapid Commun. Mass Sp.*, 24, 621–633, doi:10.1002/rcm.4429, 2010a. 11281, 11282, 11283, 11284, 11285, 11286, 11287, 11288, 11290, 11293, 11300, 11302
- Bock, M., Schmitt, J., Möller, L., Spahni, R., Blunier, T., and Fischer, H.: Hydrogen isotopes preclude marine hydrate CH_4 emissions at the onset of Dansgaard-Oeschger Events, *Science*, 328, 1686–1689, 2010b. 11281, 11291, 11292

Improving accuracy and precision of $\delta D(CH_4)$ analyses

M. Bock et al.

Title Page

Abstract

Introduction

Conclusions

References

Tables

Figures

◀

▶

◀

▶

Back

Close

Full Screen / Esc

Printer-friendly Version

Interactive Discussion



Brass, M. and Röckmann, T.: Continuous-flow isotope ratio mass spectrometry method for carbon and hydrogen isotope measurements on atmospheric methane, *Atmos. Meas. Tech.*, 3, 1707–1721, doi:10.5194/amt-3-1707-2010, 2010. 11286

Clark, P. U., Dyke, A. S., Shakun, J. D., Carlson, A. E., Clark, J., Wohlfarth, B., Mitrovica, J. X., Hostetler, S. W., and McCabe, A. M.: The last glacial maximum, *Science*, 325, 710–714, doi:10.1126/science.1172873, 2009. 11282

Dlugokencky, E. J., Steele, L. P., Lang, P. M., and Masarie, K. A.: Atmospheric methane at Mauna Loa and Barrow observatories: presentation and analysis of in situ measurements, *J. Geophys. Res.*, 100, 23103–23113, doi:10.1029/95JD02460, 1995. 11280

Ferretti, D. F., Miller, J. B., White, J. W. C., Etheridge, D. M., Lassey, K. R., Lowe, D. C., Meure, C. M. M., Dreier, M. F., Trudinger, C. M., van Ommen, T. D., and Langenfelds, R. L.: Unexpected changes to the global methane budget over the past 2000 years, *Science*, 309, 1714–1717, 2005. 11281

Fischer, H., Behrens, M., Bock, M., Richter, U., Schmitt, J., Loulergue, L., Chappellaz, J., Spahni, R., Blunier, T., Leuenberger, M., and Stocker, T. F.: Changing boreal methane sources and constant biomass burning during the last termination, *Nature*, 452, 864–867, doi:10.1038/nature06825, 2008. 11281

IPCC (Intergovernmental Panel on Climate Change): *Climate Change 2007 – The Physical Science Basis: Working Group I Contribution to the Fourth Assessment Report of the IPCC (Climate Change 2007)*, Cambridge University Press, available at: <http://www.worldcat.org/isbn/0521705967> (last access: 18 December 2013), 2007. 11280

Kennett, J. P., Cannariato, K. G., and Hendy, I. L., and Behl, R. J.: *Methane Hydrates in Quaternary Climate Change: The Clathrate Gun Hypothesis*, AGU Special Publication, 2003. 11281

Kirschke, S., Bousquet, P., Ciais, P., Saunois, M., Canadell, J. G., Dlugokencky, E. J., Bergamaschi, P., Bergmann, D., Blake, D. R., Bruhwiler, L., Cameron-Smith, P., Castaldi, S., Chevallier, F., Feng, L., Fraser, A., Heimann, M., Hodson, E. L., Houweling, S., Josse, B., Fraser, P. J., Krummel, P. B., Lamarque, J.-F., Langenfelds, R. L., Le Quere, C., Naik, V., O'Doherty, S., Palmer, P. I., Pison, I., Plummer, D., Poulter, B., Prinn, R. G., Rigby, M., Ringeval, B., Santini, M., Schmidt, M., Shindell, D. T., Simpson, I. J., Spahni, R., Steele, L. P., Strode, S. A., Sudo, K., Szopa, S., van der Werf, G. R., Voulgarakis, A., van Weele, M., Weiss, R. F., Williams, J. E., and Zeng, G.: Three decades of global methane sources and sinks, *Nat. Geosci.*, 6, 813–823, doi:10.1038/ngeo1955, 2013. 11280

**Improving accuracy
and precision of
 $\delta D(CH_4)$ analyses**

M. Bock et al.

Title Page

Abstract

Introduction

Conclusions

References

Tables

Figures

◀

▶

◀

▶

Back

Close

Full Screen / Esc

Printer-friendly Version

Interactive Discussion



Louergue, L., Schilt, A., Spahni, R., Masson-Delmotte, V., Blunier, T., Lemieux, B., Barnola, J.-M., Raynaud, D., Stocker, T. F., and Chappellaz, J.: Orbital and millennial-scale features of atmospheric CH_4 over the past 800 000 years, *Nature*, 453, 383–386, doi:10.1038/nature06950, 2008. 11280, 11282

5 Meier-Augenstein, W.: Applied gas chromatography coupled to isotope ratio mass spectrometry, *J. Chromatogr. A*, 842, 351–371, 1999. 11284

Meier-Augenstein, W., Kemp, H. F., and Lock, C. M.: N_2 : a potential pitfall for bulk 2H isotope analysis of explosives and other nitrogen-rich compounds by continuous-flow isotope-ratio mass spectrometry, *Rapid Commun. Mass Sp.*, 23, 2011–2016, doi:10.1002/rcm.4112, 2009. 11289

10 Mischler, J. A., Sowers, T. A., Alley, R. B., Battle, M., McConnell, J. R., Mitchell, L., Popp, T., Sofen, E., and Spencer, M. K.: Carbon and hydrogen isotopic composition of methane over the last 1000 years, *Global Biogeochem. Cy.*, 23, GB4024, doi:10.1029/2009GB003460, 2009. 11281, 11288

15 Mitchell, L. E., Brook, E. J., Sowers, T., McConnell, J. R., and Taylor, K.: Multidecadal variability of atmospheric methane, 1000–1800 C.E., *J. Geophys. Res.*, 116, G02007, doi:10.1029/2010JG001441, 2011. 11280

Möller, L., Sowers, T., Bock, M., Spahni, R., Behrens, M., Schmitt, J., Miller, H., and Fischer, H.: Independent variations of CH_4 emissions and isotopic composition over the past 160 000 years, *Nat. Geosci.*, 6, 885–890, doi:10.1038/ngeo1922, 2013. 11281

20 Poss, C.: Untersuchung der Variabilität des atmosphärischen Methanhaushalts hochpolarer Breiten anhand eines regionalen Trajektorienmodells und der Messung stabiler Isotope, Ph.D. thesis, University of Heidelberg, 2003. 11287

Potter, J. and Siemann, M. G.: A new method for determining $\delta^{13}C$ and δD simultaneously for CH_4 by gas chromatography/continuous-flow isotope-ratio mass spectrometry, *Rapid Commun. Mass Sp.*, 18, 175–180, doi:10.1002/rcm.1311, 2004. 11286

25 Quay, P., Stutsman, J., Wilbur, D., Snover, A., Dlugokencky, E., and Brown, T.: The isotopic composition of atmospheric methane, *Global Biogeochem. Cy.*, 13, 445–461, doi:10.1029/1998GB900006, 1999. 11281

30 Sapart, C. J., van der Veen, C., Vigano, I., Brass, M., van de Wal, R. S. W., Bock, M., Fischer, H., Sowers, T., Buizert, C., Sperlich, P., Blunier, T., Behrens, M., Schmitt, J., Seth, B., and Röckmann, T.: Simultaneous stable isotope analysis of methane and nitrous oxide on

Improving accuracy and precision of $\delta D(CH_4)$ analyses

M. Bock et al.

Title Page

Abstract

Introduction

Conclusions

References

Tables

Figures

◀

▶

◀

▶

Back

Close

Full Screen / Esc

Printer-friendly Version

Interactive Discussion



ice core samples, *Atmos. Meas. Tech.*, 4, 2607–2618, doi:10.5194/amt-4-2607-2011, 2011. 11281

Sapart, C. J., Monteil, G., Prokopiou, M., van de Wal, R. S. W., Kaplan, J. O., Sperlich, P., Krumhardt, K. M., van der Veen, C., Houweling, S., Krol, M. C., Blunier, T., Sowers, T., Martinerie, P., Witrant, E., Dahl-Jensen, D., and Röckmann, T.: Natural and anthropogenic variations in methane sources during the past two millennia, *Nature*, 490, 85–88, doi:10.1038/nature11461, 2012. 11281

Schmitt, J.: A sublimation technique for high-precision $\delta^{13}C$ on CO_2 and CO_2 mixing ratio from air trapped in deep ice cores, Ph.D. thesis, University of Bremen, 2006. 11283

Schmitt, J., Glaser, B., and Zech, W.: Amount-dependent isotopic fractionation during compound-specific isotope analysis, *Rapid Commun. Mass Sp.*, 17, 970–977, doi:10.1002/rcm.1009, 2003. 11286

Schmitt, J., Seth, B., Bock, M., van der Veen, C., Möller, L., Sapart, C. J., Prokopiou, M., Sowers, T., Röckmann, T., and Fischer, H.: On the interference of Kr during carbon isotope analysis of methane using continuous-flow combustion–isotope ratio mass spectrometry, *Atmos. Meas. Tech.*, 6, 1425–1445, doi:10.5194/amt-6-1425-2013, 2013a. 11288, 11289, 11290, 11291

Schmitt, J., Seth, B., Bock, M., and Fischer, H.: Online technique for isotope and mixing ratios of CH_4 , N_2O , Xe and mixing ratios of organic trace gases on a single ice core sample, *Atmos. Meas. Tech. Discuss.*, submitted, 2013b. 11285

Sowers, T.: Late quaternary atmospheric CH_4 isotope record suggests marine clathrates are stable, *Science*, 311, 838–840, doi:10.1126/science.1121235, 2006. 11281

Sowers, T.: Atmospheric methane isotope records covering the Holocene period, *Quaternary Sci. Rev.*, 29, 213–221, 2010. 11281, 11288

Sperlich, P., Guillevic, M., Buizert, C., Jenk, T. M., Sapart, C. J., Schaefer, H., Popp, T. J., and Blunier, T.: A combustion setup to precisely reference $\delta^{13}C$ and δ^2H isotope ratios of pure CH_4 to produce isotope reference gases of $\delta^{13}C-CH_4$ in synthetic air, *Atmos. Meas. Tech.*, 5, 2227–2236, doi:10.5194/amt-5-2227-2012, 2012. 11287

Walter, K. M., Chanton, J. P., Chapin III, F. S., Schuur, E. A. G., and Zimov, S. A.: Methane production and bubble emissions from arctic lakes: isotopic implications for source pathways and ages, *J. Geophys. Res.*, 113, G00A08, doi:10.1029/2007JG000569, 2008. 11288

Werner, R. A. and Brand, W. A.: Referencing strategies and techniques in stable isotope ratio analysis, *Rapid Commun. Mass Sp.*, 15, 501–519, doi:10.1002/rcm.258, 2001. 11289

Improving accuracy and precision of $\delta D(\text{CH}_4)$ analyses

M. Bock et al.

Table 1. Precision of the new $\delta D(\text{CH}_4)$ system. Mean values are given in column 3; columns 4 and 5 show standard deviations (1σ) of samples and “Air Controlé” reference air measurements, respectively. Columns 6–8 show values obtained with the previous set-up presented in Bock et al. (2010a). “Air Controlé” measurements are used to calibrate the samples to the international VSMOW scale. “N” represents the number of measurements used. Ice sample results are not corrected for any firn diffusion process. Gas ages of the ice samples are estimated as follows: B30: 670 aBP, B34: 1500 aBP, WAIS: 410 aBP. The WAIS samples are from core WDC05A, tube 184, depth range: 172.74–173.03 m. NGRIP gas samples date from between 870 and 9000 aBP.

sample description (sample size, origin CH_4 concentration)	this study			Bock et al. (2010a)			
	<i>N</i>	$\delta D(\text{CH}_4)$ (‰)	1σ sample (‰)	1σ reference (‰)	<i>N</i>	$\delta D(\text{CH}_4)$ (‰)	1σ sample (‰)
Air reference and samples							
Air Controlé (all injections, 4–40 mL)	544	−93.6	1.3		343	−93.6	2.8
Air Controlé (only larger loops (18–40 mL)	69	−93.6	0.8		86	−93.5	2.3
Saphir 4 ($[\text{CH}_4] = 761$ ppb)	36	−171.6	1.2		0.9		
Saphir 4 (loop after sample)	34	−173.2	1.4	0.9			
Saphir 3 ($[\text{CH}_4] = 1004$ ppb)	2	−173.4	0.4	0.9	18	−167.6	2.4
Boulder (CAO8289 $[\text{CH}_4] = 1500$ ppb)	14	−81.0	1.1	0.7	8	−80.8	1.3
NAT-332 ($[\text{CH}_4] = 2141$ ppb)	3	−108.0	1.8	0.8	6	−106.3	1.2
Dome 6 (firn air $[\text{CH}_4] = 1718$ ppb)	2	−71.0	0.8	0.2	2	−71.0	0.1
Ice core samples							
B30 (Greenland, preindustrial, depth range 2 m)	2	−91.5	0.8	1.1	14	−94.7	−3.7
WAIS (Antarctica, preindustrial, parallel replicates)	4	−73.0	0.5	1.2			
B34 (Antarctica, late Holocene, depth range 9 m)	47	−74.6	2.8	1.5			
Ice core replicates							
B34 ice (parallel replicates, late Holocene)	35	depth intervals	pooled 1σ				
NGRIP (bag replicates of gas cut, Holocene)	27	16	2.2				
		13	2.3				

Table 2. Results of ice core samples from B34. Given depth is the middle of each sample. Depending on replicate shape and weight typical samples are between 5 and 15 cm long. The standard deviation of Air Controlé measurements used to calibrate the sample is given in the column named 1σ . Samples with a weight < 220 g correspond to a methane amount comparable to samples from the glacial with lowest CH₄ concentration of around 350 ppb.

middle depth (m)	measurement date (Day Month Year)	$\delta D(CH_4)$ (‰)	1σ (‰)	weight (g)
181.435	20 Feb 2013	-74.8	0.9	219.6
181.553	22 Feb 2013	-75.6	0.9	200.4
181.935	21 Feb 2013	-76.7	0.9	199.4
181.935	12 Mar 2013	-75.0	0.9	200.4
183.065	2 Nov 2011	-79.0	1.9	202.3
183.065	3 Nov 2011	-73.6	1.9	209.7
183.128	8 Nov 2011	-74.1	2.6	206.5
183.190	15 Feb 2012	-76.2	2.7	316.7
183.190	3 Nov 2011	-76.6	1.9	202.2
183.315	7 Mar 2012	-77.1	1.6	261.3
183.315	16 Feb 2012	-79.2	2.7	210.4
183.445	1 Nov 2011	-75.5	1.9	377.0
183.445	22 Feb 2012	-78.8	3.3	264.4
183.570	8 Dec 2011	-77.2	2.1	312.6
183.695	31 Oct 2011	-78.4	1.9	394.3
183.825	30 Sep 2011	-78.8	1.2	349.1
183.825	28 Sep 2011	-74.6	1.2	376.5
183.830	11 Sep 2013	-76.8	1.2	254.6
183.830	18 Jul 2013	-75.5	1.4	293.3
183.830	20 Aug 2013	-73.6	1.8	298.8
183.830	13 Sep 2013	-73.3	1.2	267.6
183.945	10 Feb 2012	-73.7	2.7	318.5
184.060	5 Aug 2013	-75.1	1.7	232.2
184.380	26 Jul 2013	-71.6	1.4	224.4
184.550	12 Jul 2013	-70.9	0.9	250.6
184.550	19 Aug 2013	-72.2	1.8	259.0
184.730	13 Jun 2013	-76.3	1.2	211.6
184.730	7 Jun 2013	-75.2	1.2	257.0
184.910	18 Jun 2013	-70.9	1.1	251.5
184.910	6 Jun 2013	-74.2	1.2	239.8
185.190	18 Jul 2011	-74.5	1.2	223.8
185.190	18 Jul 2011	-77.5	1.2	212.9
185.338	15 Jul 2011	-73.9	1.2	446.0
185.338	15 Jul 2011	-73.3	1.2	427.6
185.500	26 Apr 2011	-75.3	0.4	427.0
186.985	19 Mar 2013	-72.3	0.9	408.6
187.133	19 Feb 2013	-71.6	0.9	310.0
187.420	24 Oct 2012	-70.9	1.9	347.4
187.420	23 Oct 2012	-74.2	1.9	340.7
190.475	31 May 2013	-68.7	1.2	261.7
190.475	4 Jun 2013	-68.0	1.2	251.4
190.565	30 May 2013	-70.1	1.2	262.3
190.565	22 May 2013	-71.3	1.2	250.7
190.655	17 May 2013	-76.9	1.1	264.4
190.775	5 Jun 2013	-80.2	1.2	205.1
190.775	15 May 2013	-73.9	1.0	229.4
190.775	8 May 2013	-72.9	0.5	245.1

Improving accuracy and precision of $\delta D(CH_4)$ analyses

M. Bock et al.

Title Page

Abstract Introduction

Conclusions References

Tables Figures

⏪ ⏩

◀ ▶

Back Close

Full Screen / Esc

Printer-friendly Version

Interactive Discussion



Improving accuracy and precision of $\delta D(\text{CH}_4)$ analyses

M. Bock et al.

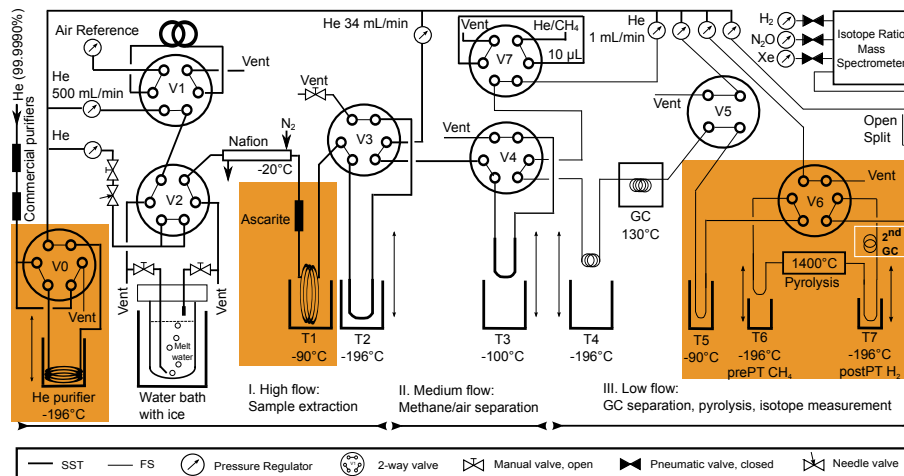


Fig. 1. Flow scheme of the new $\delta D(\text{CH}_4)$ system including pre and post pyrolysis trapping of methane and hydrogen, respectively, and a short second chromatographic separation column (2nd GC). The orange areas highlight the major differences from Bock et al. (2010a).

Title Page

Abstract

Introduction

Conclusions

References

Tables

Figures

◀

▶

◀

▶

Back

Close

Full Screen / Esc

Printer-friendly Version

Interactive Discussion



Improving accuracy
and precision of
 $\delta D(CH_4)$ analyses

M. Bock et al.

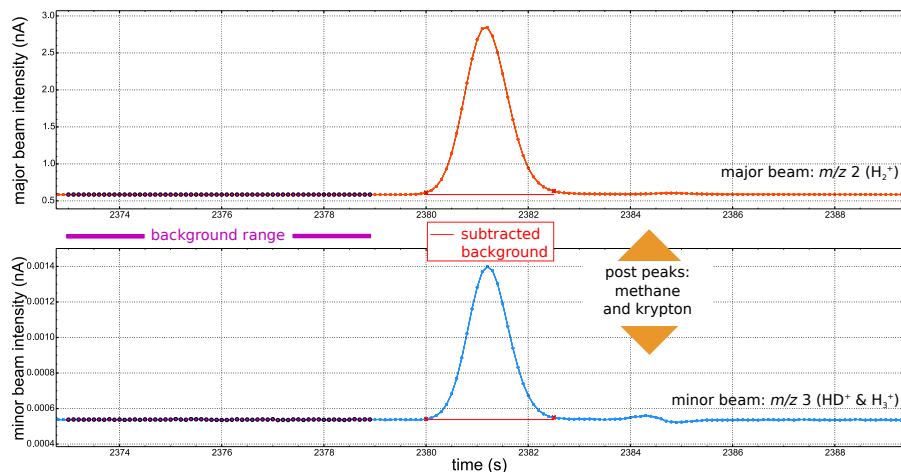


Fig. 2. Chromatogram of a CH_4 derived H_2 peak of an ice core sample (B34). Peak integration limits are shown as red crosses. The data range used for the background determination is shown as magenta bullets and the subtracted background values as red line. Also indicated is the data range after the sample peak where we observe two post peaks, namely not pyrolyzed methane and krypton (compare text and Fig. 3).

Title Page

Abstract

Introduction

Conclusions

References

Tables

Figures

◀

▶

◀

▶

Back

Close

Full Screen / Esc

Printer-friendly Version

Interactive Discussion

Improving accuracy and precision of $\delta D(\text{CH}_4)$ analyses

M. Bock et al.

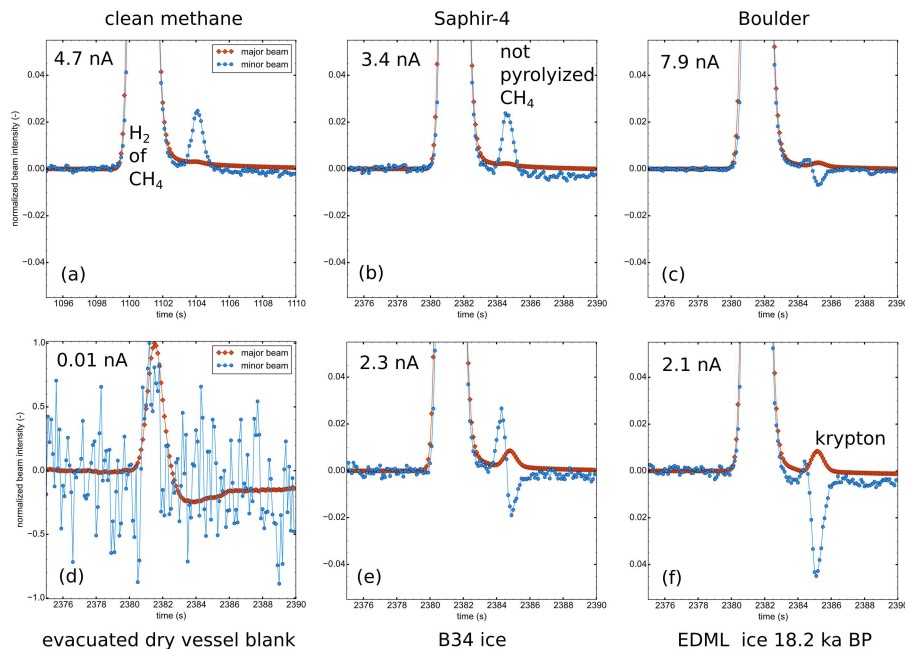


Fig. 3. Chromatograms showing CH_4 -derived H_2 peaks and post peaks (methane and krypton). Peak data are normalized to the H_2 maximum, which is given in (nA) in the top left corner of each subplot. Shown are (a) a clean CH_4 injection (via V7), (b) Saphir-4 (artificial clean air mixture (no Kr and 761 ppb CH_4)), (c) Boulder (natural air with reduced CH_4 (1500 ppb) and ambient Kr), (d) pure helium extraction of an evacuated dry sample cylinder, (e) B34 ice (ambient Kr, about 630 ppb CH_4 , dry drilled next to EDML, the EPICA (European Project for Ice Coring in Antarctica) drill site in Dronning Maud Land, Antarctica: gas age is 1500 aBP and (f) EDML ice (ambient Kr, about 370 ppb CH_4): gas age is 18.2 ka BP.

Title Page

Abstract

Introduction

Conclusions

References

Tables

Figures

◀

▶

◀

▶

Back

Close

Full Screen / Esc

Printer-friendly Version

Interactive Discussion

Improving accuracy
and precision of
 $\delta D(\text{CH}_4)$ analyses

M. Bock et al.

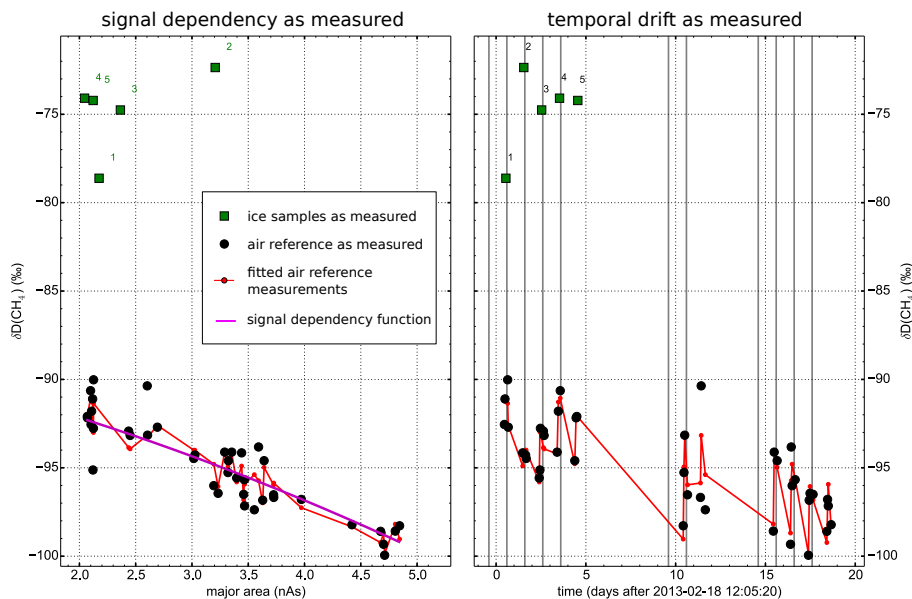


Fig. 4. Uncalibrated $\delta D(\text{CH}_4)$ data of our reference Air Controlé (black bullets) and B34 ice core samples (green squares). The left panel shows $\delta D(\text{CH}_4)$ vs. major area, i.e. the observed signal dependency. The magenta line indicates the polynomial correction function for signal dependency. The right panel shows the same uncalibrated data plotted against time. The red dots and line show the fitted standard numbers, which are later used to calibrate the samples, as described in the Appendix. The closer the red and black symbols are to each other, the better the fit.

Title Page

Abstract

Introduction

Conclusions

References

Tables

Figures

◀

▶

◀

▶

Back

Close

Full Screen / Esc

Printer-friendly Version

Interactive Discussion

Improving accuracy
and precision of
 $\delta D(\text{CH}_4)$ analyses

M. Bock et al.

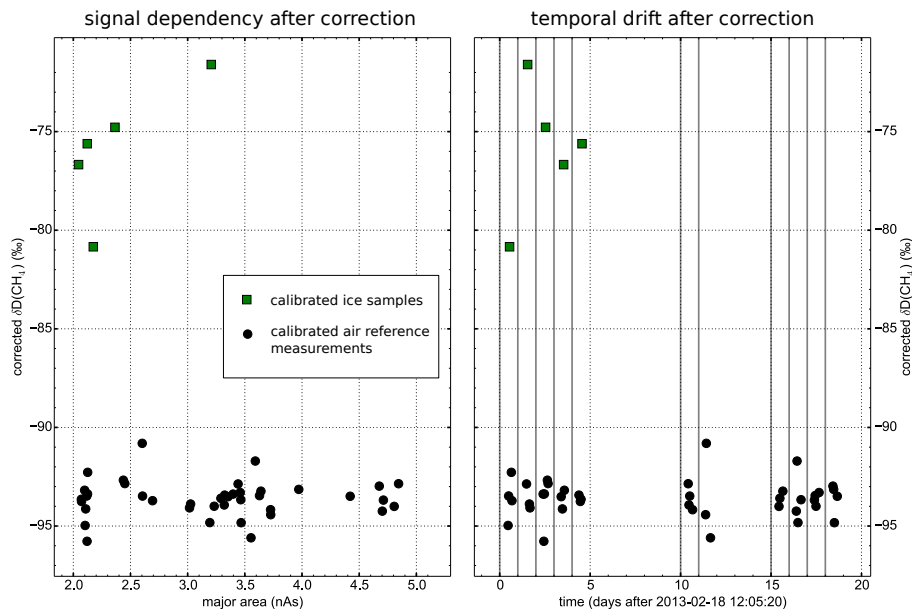


Fig. 5. Calibrated $\delta D(\text{CH}_4)$ data of Fig. 4 after correction for temporal drift and signal dependency. The left panel shows $\delta D(\text{CH}_4)$ vs. major area and the right panel shows the same data plotted against time. Black bullets show standard measurements (Air Controlé), green squares show B34 ice core samples.

[Title Page](#)[Abstract](#)[Introduction](#)[Conclusions](#)[References](#)[Tables](#)[Figures](#)[◀](#)[▶](#)[◀](#)[▶](#)[Back](#)[Close](#)[Full Screen / Esc](#)[Printer-friendly Version](#)[Interactive Discussion](#)

